

MONTE CARLO SIMULATION OF INTERLAYER MOLECULAR STRUCTURE IN SWELLING CLAY MINERALS. 2. MONOLAYER HYDRATES

N. T. SKIPPER,¹ GARRISON SPOSITO,² AND FANG-RU CHOU CHANG²

¹ Department of Physics and Astronomy, University College, Gower Street, London WC1E 6BT, UK

² Department of Environmental Science, Policy, and Management
University of California, Berkeley, California 94720-3110

Abstract—Monte Carlo (MC) simulations of interlayer molecular structure in monolayer hydrates of Na-saturated Wyoming-type montmorillonites and vermiculite were performed. Detailed comparison of the simulation results with experimental diffraction and thermodynamic data for these clay-water systems indicated good semiquantitative to quantitative agreement. The MC simulations revealed that, in the monolayer hydrate, interlayer water molecules tend to increase their occupation of the midplane as layer charge increases. As the percentage of tetrahedral layer charge increases, water molecules are induced to interact with the siloxane surface O atoms through hydrogen bonding and Na⁺ counter-ions are induced to form inner-sphere surface complexes. These results suggest the need for careful diffraction experiments on a series of monolayer hydrates of montmorillonite whose layer charge and tetrahedral isomorphous substitution charge vary systematically.

Key Words—Clay water systems, Monte Carlo simulation, swelling clays.

INTRODUCTION

The molecular structure of water and the distribution of counter-ions at the clay-water interface remain topics of great interest and controversy in colloid science (Newman 1987, Güven 1992). A fundamental but unresolved issue is the extent to which counter-ions determine the organization of interlayer water molecules in smectite-water systems (Sposito 1984, Low 1985, 1987). This issue is particularly acute in the case of Na⁺ counterions, and compelling arguments have been made for both a dominant role (Sposito 1992) and a negligible influence (Miller and Low 1990) of adsorbed Na⁺ in the development of montmorillonite interlayer properties. On the molecular level, these two opposing perspectives come down to a determination of whether interlayer water is similar to an aqueous ionic solution or to an epitaxial condensed phase (Sposito and Prost 1982).

In the study of the molecular structure of bulk liquid water and aqueous electrolyte solutions, Monte Carlo (MC) simulation has proven to be a valuable heuristic technique (Beveridge *et al* 1983, Bopp 1987). The philosophy of this approach is to construct a convenient mathematical description of molecular interactions represented as potential functions, then sample the configuration of a manageable system of molecules so described to ascertain its equilibrium properties (Allen and Tildesley 1987). Comparison of the results with empirical data not only tests the success with which the molecular interactions have been captured by model potential functions, but also points to important new experiments that are needed to close gaps in under-

standing. Bleam (1993) has reviewed the few published MC simulations of interlayer structure and noted their evolution from rather primitive concepts of water-water and clay-water interactions to fairly realistic modeling of both these interactions and the equally important counter-ion-water and counter-ion-clay mineral interactions. Skipper *et al* (1991b, 1993) have performed three-dimensional MC simulations of high-charge, trioctahedral or dioctahedral smectites bearing either one or two monolayers of adsorbed water and either Mg²⁺ or Na⁺ as counter-ions. Their results for a Na-saturated, trioctahedral smectite bearing only octahedral layer charge and two monolayers of water indicated that Na⁺ formed both inner-sphere and outer-sphere surface complexes, and that interlayer water molecules were not well organized around Na⁺ cations, but interacted significantly through hydrogen bonding among themselves and with the clay mineral. The same picture emerged from their MC simulations of Na-saturated, dioctahedral smectite bearing only tetrahedral layer charge and either one or two monolayers of water. These results may reflect the middling influence of Na⁺ on water molecules in aqueous solution, where its status falls between the strongly-solvating Li⁺ and the innocuous K⁺ (Madden and Impey 1986).

In a companion paper, Skipper *et al* (1995) have outlined and tested a methodology for extending MC simulations to hydrates of dioctahedral smectites bearing both tetrahedral and octahedral layer charge (e.g., Wyoming-type montmorillonites). Their analysis indicated that the development of potential functions for interlayer species could be based on the MCY model (Matsouka *et al* 1976) of water-water interactions, and

that a simulation domain covering about eight unit cells of a clay mineral layer could be used successfully with periodic boundary conditions to approximate the behavior of macroscopic clay layers.

In the present paper, this methodology is applied to simulate interlayer molecular structure in the dehydrated forms and in monolayer hydrates of Wyoming-type montmorillonites bearing Na^+ counter-ions. The objectives of the simulations were to examine the accuracy of the model potential functions by comparisons with the wealth of experimental data for low hydrates of Na-montmorillonite (Sposito 1984), and to elucidate the role of tetrahedral vs. octahedral layer charge in organizing interlayer structure. This second objective was given additional focus by simulations of monolayer hydrates of the montmorillonites without tetrahedral layer charge and of trioctahedral vermiculite, for which detailed information is available concerning the interlayer region from X-ray and neutron diffraction experiments (de la Calle *et al* 1984, Skipper *et al* 1991a).

METHODS

Model monolayer hydrates

Two important subgroups of 2:1 layer-type clay minerals were investigated by MC simulation, dioctahedral smectite and trioctahedral vermiculite. The unit-cell formula of Na-saturated dioctahedral smectite is (Sposito 1984):



where $x \equiv 12 - a - b$ is the layer charge and Na^+ is the balancing counter-ion. Smectites are defined by x in the range 0.50–1.2, and those for which $x < 0.85$ with $(8-a)/x$ in the range 0.15–0.50 are termed Wyoming-type montmorillonite (Schulz 1969, Newman and Brown 1987). Two model Wyoming-type montmorillonites were simulated, one with $x = 0.72$, $(8-a)/x = 0.33$, and one with $x = 0.48$, $(8-a)/x = 0.50$, corresponding to a medium- and a low-charge Wyoming-type montmorillonite, respectively. In order to examine the effects of layer charge arising in the tetrahedral sheet (from isomorphous substitutions), model smectites with $x = 0.48$ or 0.72 and $a = 8$ (i.e., zero tetrahedral charge) also were simulated. [These model montmorillonites might be thought of as *hypothetical* “low-charge” Otay-type montmorillonite, since the latter is defined normally by $(8-a)/x < 0.15$, but $x > 0.85$ (Schulz 1969, Newman and Brown 1987).]

The unit-cell formula of trioctahedral vermiculite is:



where $x = 8-a$ is now the layer charge and Na^+ is again the counter-ion. In the present study, $x = 1.5$, in the middle of the defining range, $1.2 < x < 1.8$ (Sposito

1984) and typical of the well-known Llano vermiculite (Newman and Brown 1987). As in the case of the model montmorillonites, the effects of tetrahedral charge were examined by simulation of a model vermiculite with $a = 8$ (i.e., talc).

Model monolayer hydrates of the Na-saturated clay minerals were assumed to contain about four water molecules per unit cell, corresponding to a gravimetric water content of about 0.1 g water/g clay (Newman 1987).

Monte Carlo simulations

Monte Carlo (MC) simulations were performed on the Cray Y-MP8/864 at the San Diego Supercomputer center using the program MONTE (Skipper 1992). Both dehydrated forms and monolayer hydrates of the clay minerals were simulated.

General principles of Monte Carlo simulation for liquids are discussed by Allen and Tildesley (1987), and a detailed review of the issues that pertain to the Monte Carlo simulation of liquid water molecular structure is given by Beveridge *et al* (1983). The methodology as applied to interlayer water and clay minerals is described by Skipper *et al* (1994). In this latter paper, justification is given for the choices of potential functions and simulation cell properties. The potential function used for water-water interactions is the widely-adopted MCY potential (Matsouka *et al* 1976), which has been shown to perform very well in comparative studies of MC simulations of liquid water (Beveridge *et al* 1983). The simulation cell selected is $21.12 \text{ \AA} \times 18.28 \text{ \AA}$ (about eight unit cells). Periodic boundary conditions are imposed, and the long-range part of the coulomb interactions among ions is calculated by the three-dimensional Ewald sum method (Allen and Tildesley 1987).

Simulations were conducted for $T = 300 \text{ K}$, $\sigma_{zz} = 10^5 \text{ Pa}$ (σ_{zz} = stress applied normal to the clay mineral layers), and a fixed number of ($\text{Na}^+ + \text{H}_2\text{O}$) in the interlayer region. For the monolayer hydrates of montmorillonite, this latter number was 38, with the number of Na^+ being 4 or 6 for $x = 0.48$ or 0.72 . For the monolayer hydrate of talc, it was also 38 (no counterion Na^+), whereas for vermiculite it was 44 (12 Na^+). Thus, the MC simulation ensemble represents an isothermal, isobaric, closed clay-water system (Skipper *et al* 1994). Some layer-charge and hydration properties of the model clay minerals are listed in Table 1.

For each clay-water system containing a 21.12 \AA by 18.28 \AA simulation cell, MC equilibration was as follows. First, 5000 moves were attempted in which only the water molecules were selected. This was followed by about 150,000 attempted moves in which all molecules could be chosen. Equilibration was judged to have taken place when the average potential energy and the z -dimension of the simulation cell had reached

Table 1. Layer charge and calculated layer spacing for model 2:1 clay minerals.

Layer charge (x)	Tetrahedral charge (%)	Layer spacing, dry (Å)	Layer spacing, hydrated (Å)
0.72	0.0	9.21 ± 0.02	11.94 ± 0.04 ²
0.72	33.3	9.85 ± 0.02	12.08 ± 0.05 ²
0.48	0.0	9.19 ± 0.02	12.51 ± 0.08 ³
0.48	50.0	9.88 ± 0.02	12.55 ± 0.08 ³
0.00 ¹	0.0	9.10 ± 0.02	13.2 ± 0.24
1.5 ¹	100.0	9.96 ± 0.03	11.60 ± 0.04 ³

¹ Trioctahedral clay mineral.

² 3.8 H₂O/unit cell (8.95 Å × 5.17 Å for montmorillonite).

³ 4.0 H₂O/unit cell (9.23 Å × 5.26 Å for vermiculite).

⁴ 4.8 H₂O/unit cell (9.18 Å × 5.29 Å for talc).

constant values. The simulations then were allowed to proceed for at least an additional 200,000 moves. Data were collected for averaging every 200 attempted moves.

Interlayer density profiles for Na⁺, O, and H were calculated from the MC simulation data using the equations:

$$\rho_{\text{Na}}(z) = (z_L/N_{\text{Na}})dn_{\text{Na}}/dz \quad (1)$$

$$\rho_{\text{O}}(z) = (29.89/A)dn_{\text{O}}/dz \quad (2)$$

$$\rho_{\text{H}}(z) = (59.78/A)dn_{\text{H}}/dz \quad (3)$$

where dn is the number of atoms of a given species between planes at z and $z + dz$, z_L is the equilibrium layer spacing in Å (equivalent to the d -spacing measured by X-ray diffraction), $N_{\text{Na}} = 4, 6, \text{ or } 12$ is the number of Na⁺ per simulation cell of area $A = 386.0736 \text{ \AA}^2$. The numerical coefficients in Equations 2 and 3 are, respectively, the inverses of the number densities of O or H atoms in bulk liquid water, expressed per Å³ (z is in Å). Thus, the Na⁺ profile is relative to the number density of Na⁺ in the simulation cell (N_{Na}/Az_L), whereas the O and H profiles are relative to bulk water.

Radial distribution functions were computed from the simulation data using the equation (Allen and Tildesley 1987):

$$g_{\alpha\beta}(r) = (1/4\pi\rho_{\beta}r^2)dn_{\beta}/dr \quad (4)$$

where dn_{β} is the number of β -atoms between spherical shells at r and $r + dr$ centered on the α -atom, and ρ_{β} is the number density of β -atoms in the simulation cell at equilibrium. In the present study, $g_{\text{NaO}}(r)$, $g_{\text{OO}}(r)$, and $g_{\text{OH}}(r)$ were calculated. They describe relative fluctuations in the density of O or H atoms relative to a central Na or O atom, and to the average density of O or H atoms. The integral,

$$4\pi\rho_{\beta} \int_0^R g_{\alpha\beta}(r)r^2 dr = n_{\alpha\beta}(R) \quad (5)$$

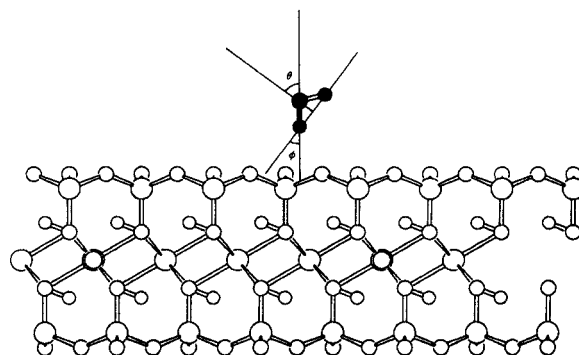


Figure 1. Orientation of a water molecule relative to a neighboring siloxane surface, to illustrate the definitions of the angles θ and ϕ .

gives the running coordination number of β -atoms about the central α -atom as a function of the separation R (Beveridge *et al* 1983).

To describe the orientation of interlayer water molecules, we define distributions of the dipole moment vector and H-H axis vector, relative to the normal to the closest siloxane surface (angles θ and ϕ in Figure 1), through the distribution functions:

$$P(\theta) = (1/N_w r)dn(\theta)/d\theta \quad (6)$$

$$(N_w = 32, 34, \text{ or } 38)$$

$$P(\phi) = (1/N_w)dn(\phi)/d\phi \quad (7)$$

where dn is the number of dipole moment vectors or H-H axis vectors oriented at angles in the range θ to $\theta + d\theta$ or ϕ to $\phi + d\phi$ and N_w is the number of water molecules in a simulation cell. We have not normalized these distributions to the solid angle by dividing $P(\theta)$ or $P(\phi)$ by $\sin(\theta)$ or $\sin(\phi)$, respectively (Beveridge *et al* 1983).

RESULTS AND DISCUSSION

Average layer spacing and potential energy

Table 1 lists values of the layer spacings for dehydrated and monolayer hydrates of six model 2:1 clay minerals as calculated by MC simulation at 300 K and 10^5 Pa. The first four rows in the table represent dioctahedral Wyoming-type (or "low-charge" Otay-type) montmorillonites (Newman and Brown 1987), while the last two rows represent talc and trioctahedral vermiculite, respectively.

For the dehydrated clay minerals, there is a distinct trend of increasing layer spacing with an increasing percentage of layer charge created by isomorphic substitution in the tetrahedral sheet (columns 2 and 3). This trend has a simple explanation in terms of the positioning of Na⁺ counter-ions in the dry clay mineral

interlayer. Layer charge arising from tetrahedral substitution is located close to the siloxane surface and Na^+ counter-ions can therefore bind to the atoms above tetrahedral Al (Sposito 1984). The octahedral substitution sites, on the other hand, lie within the layer and Na^+ counter-ions would interact rather less strongly with them except for the fact that desolvated Na^+ counter-ions can enter the hexagonal cavities of the siloxane surface, directly above the structural OH groups (Sposito *et al* 1983). A 2:1 clay mineral with no tetrahedral substitution thus should exhibit a layer spacing close to that of pyrophyllite or talc. However, if a clay mineral contains any tetrahedral layer charge, the layer spacing is increased to about 9.8 Å to accommodate the cations bound to the siloxane surface. As a general rule, we would expect the layer spacing to increase with the percentage of tetrahedral layer charge. This expectation is borne out in a comparison of d-spacings between pyrophyllite (9.2 Å; Bailey 1980) and dehydrated Wyoming-type montmorillonite (9.8 Å; Mooney *et al* 1952b, Johnston *et al* 1992), as measured by X-ray diffraction. The observed d-spacing for talc is 9.3 Å, whereas "talc-like" components of natural vermiculite exhibit a d-spacing of 9.0 Å (Bailey 1980), in good agreement with the MC simulation result (9.1 Å). A d-spacing of 9.6 Å has been reported for dehydrated Na-vermiculite (de la Calle and Suquet 1988).

The layer spacings for the monolayer hydrates of montmorillonite in Table 1 are in agreement with the d-spacings measured by X-ray diffraction for the monolayer hydrates of Wyoming-type montmorillonites (12.0–12.6 Å, Table 2). The calculated layer spacing of vermiculite in Table 1 can be compared with the d-spacings, 11.78–11.85 Å, reported for monolayer hydrates of Na-vermiculite (de la Calle *et al* 1984, Skipper *et al* 1991a).

The average potential energy per mole of interlayer water is calculated in the MC simulation as the difference between the total potential energy of the clay-water-system and the clay mineral alone, this difference then being divided by the number of moles of interlayer water. This theoretical quantity may be compared either to the isosteric heat of adsorption (or desorption), deduced from the temperature-dependence of adsorption (or desorption) isotherms; or to the sum of the heat of condensation of bulk water and the heat of immersion suitably normalized to the initial water content of the clay mineral (Adamson 1990). This comparison is only approximate, however, because of the well-known hysteresis in water vapor adsorption by clay minerals (Fu *et al* 1990). The MC simulation of interlayer water in the model Wyoming-type montmorillonites listed in Table 1 led to average potential energy values of 13.5 ± 0.1 and 11.1 ± 0.1 kcal/mole for layer charges of 0.72 and 0.48, respectively. These results may be compared to the range of isosteric heats (q_{iso}) observed for monolayer hydrates of Wyoming-

Table 2. Experimental d-spacings and "thermodynamic" data for single-layer hydrates of Wyoming-type montmorillonite.

Layer charge	d-spacing (Å)	q_{iso}^1 (kcal/mole)	q_{im}^2 (kcal/mole)	Reference
0.64	12.1	12.1	—	Mooney <i>et al</i> 1952a, 1984b)
0.64	12.0	—	1.1	Zettlemoyer <i>et al</i> (1955)
0.8 ³	—	12.5	—	Slabaugh (1959)
0.75	12.6	—	1.0	Keren and Shainberg (1975, 1980)
0.75	—	12 ⁴	—	
0.75	12.1	—	1.1	Fu <i>et al</i> 1990)

¹ Isosteric heat of adsorption or desorption.

² Heat of immersion \div initial water content.

³ Schultz (1969).

⁴ Calculated in the present study from Fig. 1 in Keren and Shainberg (1980).

type montmorillonites, 12–12.5 kcal/mole (Table 2), and to the sum of 10.5 kcal/mole (heat of condensation) plus the measured heat of immersion values (q_{im}) in Table 2, 11.5 kcal/mole. The approximate agreement is satisfactory given the conceptual uncertainty in interpreting the experimental data. For the monolayer hydrate of Na-vermiculite, van Olphen (1965) reports a heat of immersion equivalent to $q_{\text{im}} \approx 3.75 \pm 0.02$ kcal/mole; thus 14.3 kcal/mole from experiment can be compared to the calculated average potential energy value of 14.3 ± 0.1 kcal/mole obtained in the MC simulation of the model vermiculite in Table 1. Interestingly, the average potential energy of the model monolayer hydrate of talc in Table 1 was found to be 7.7 ± 0.1 kcal/mole, implying a *negative* heat of immersion and, therefore, a hydrophobic interaction of talc with water, a well-known fact (Newman 1987, Skipper *et al* 1989). Moreover, unlike bulk water simulated with the MCY potential, the simulated interlayer water in talc did not expand indefinitely under 1 bar pressure, possibly indicating an "ice-like" structure as opposed to liquid structure.

Interlayer density profiles

Interlayer density profiles for Na^+ and for O and H are shown in Figures 2 and 3, respectively. These profiles were calculated with the results of the MC simulations of the model clay minerals listed in Table 1 and the definitions in Eqs. (1–3). For both the low-charge and medium-charge model Wyoming-type montmorillonites, the Na^+ density profiles reveal two species of adsorbed cation in the monolayer hydrate. One species is an inner-sphere complex between Na^+ and surface O atoms near a site of isomorphic substitution in the tetrahedral sheet (outermost peaks in the two uppermost profiles in Figure 2). The other species is an outer-sphere complex between solvated Na^+ and the siloxane surface (inner peaks in the two uppermost profiles in Figure 2). In the absence of charge arising from the tetrahedral sheet, only outer-sphere com-

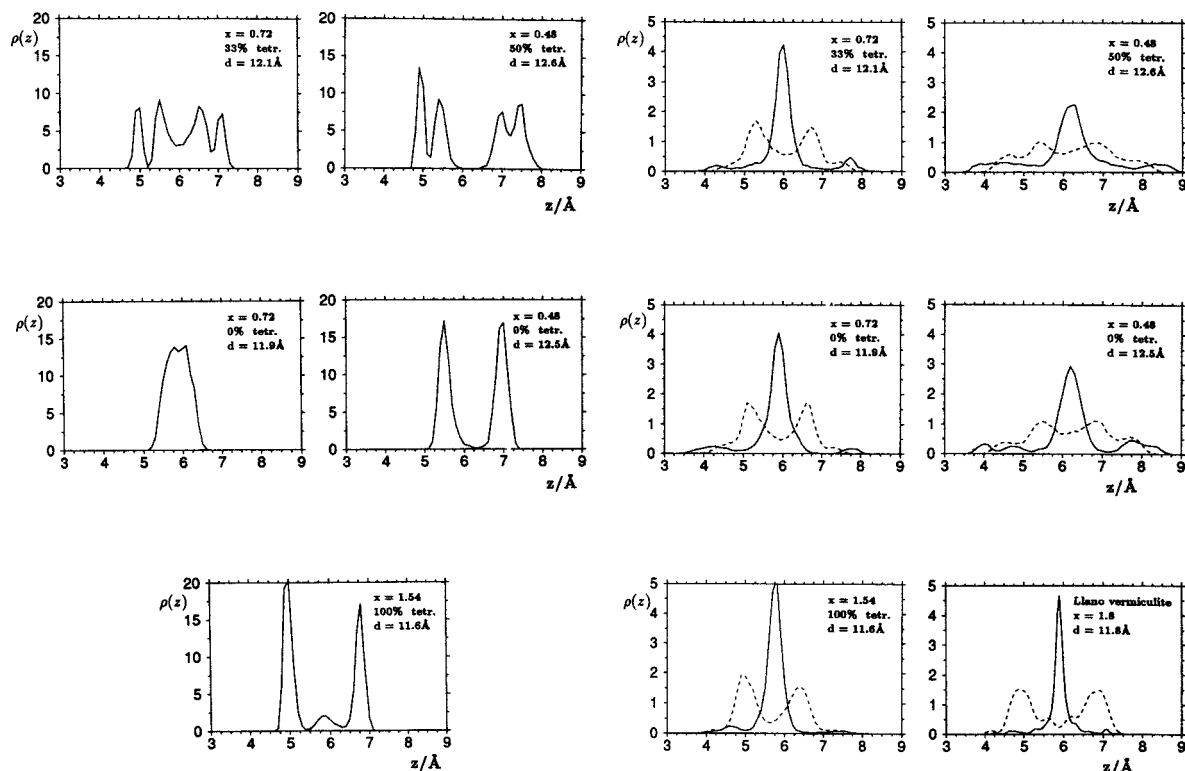


Figure 2. Graphs of $\rho_{\text{Na}}(z)$ in monolayer hydrates of Wyoming-type montmorillonites (upper two rows) and vermiculite.

plexes are found (second row of profiles in Figure 2) and, as the layer charge increases, the solvated Na^+ tend to reside in the midplane between clay mineral layers.

Sposito *et al* (1983) demonstrated by infrared spectroscopy that Na^+ counter-ions on Wyoming-type montmorillonite ($x = 0.62$) leave the hexagonal cavities in the siloxane surface to become solvated interlayer species as the clay mineral forms a monolayer hydrate (d -spacing = 12.1 \AA). Pezerat and Méring (1967) showed by Fourier analysis of X-ray diffraction patterns for a partially-formed monolayer hydrate of Wyoming-type montmorillonite ($x = 0.64$, d -spacing = 12.4 \AA) that adsorbed Na^+ remained very close to the siloxane surface as the clay mineral adsorbed water vapor. It is possible that Na^+ also contributed to the peaks in their electron density profile near the interlayer midplane, which Pezerat and Méring (1967) attributed solely to water molecules. These experimental results are in qualitative agreement with the profiles in Figure 2.

The Na^+ density profile for the model vermiculite listed in Table 1 indicates that only inner-sphere surface complexes form with the adsorbed cations. This result is expected from the trend observed for the montmorillonites, given the high tetrahedral layer charge in

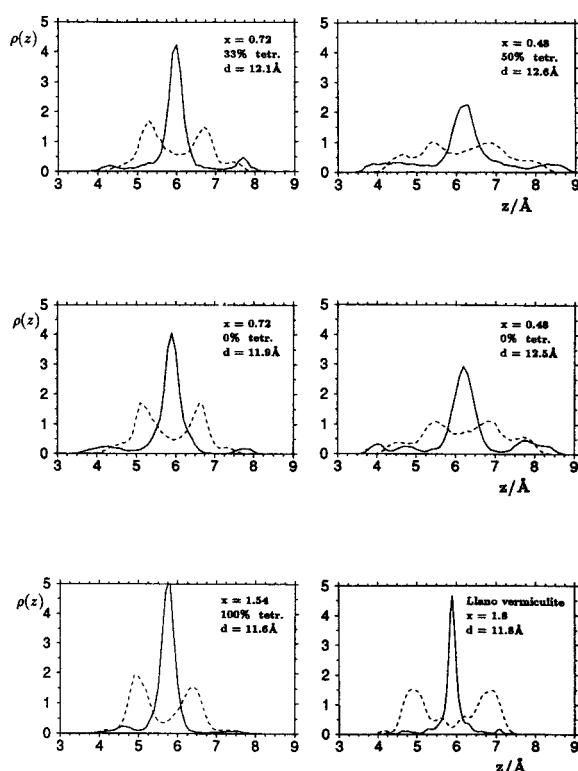


Figure 3. Graphs of $\rho_{\text{O}}(z)$ (solid curve) and $\rho_{\text{H}}(z)$ (dashed curve) for the same clay-water systems as in Figure 2.

vermiculite. The appearance of a doublet, however seems to be in contradiction with the X-ray diffraction analyses of the monolayer hydrate of Na-vermiculite published by Bradley *et al* (1963), Le Renard and Manny (1971), and de la Calle *et al* (1984), all of whom placed adsorbed Na^+ at the interlayer midplane. Skipper *et al* (1991a) made the same inference in their neutron diffraction study of 11.8 \AA Na-vermiculite. Although it is difficult to resolve diffraction peaks of interlayer Na^+ from those of water molecules, the MC simulation, which shows only a small Na^+ peak at the interlayer midplane, may overestimate the response of the counter-ions to tetrahedral charge.

This issue appears in a more subtle fashion even in the first row of density profiles in Figure 2. In nature, the distribution of isomorphous substitutions is likely to be disordered, whereas the use of a finite simulation cell and periodic boundary conditions perforce will introduce an ordering of the positions of these charge sites for a MC simulation. In preliminary runs, the effects of the positions of the charge sites on the layer spacing, average potential energy of interlayer water, and even the molecular configuration of the water were found to be insignificant, whereas for the Na^+ distribution, the opposite was true. In the case of the montmorillonites depicted in the top row of Figure 2, we would expect to find equal numbers of Na^+ in each of

the four planes (this is what we mean by “symmetric” in the following discussion). However, with “random” layer-charge distributions used in conjunction with a $21.12 \text{ \AA} \times 18.28 \text{ \AA}$ cell, we found that this counterion “symmetry” is broken. We attributed this to the particular position of the tetrahedral substitution sites (cf. the second row of profiles in Figure 2). We decided, therefore, to select more regular distributions of the charge sites, to ensure that the top and bottom halves of the clay mineral layer are equivalent (Skipper *et al* 1995). This gave cation density profiles that were, on average, “symmetric” about the midplane of the interlayer, but we noted that, even with a regular layer charge distribution, individual cation configurations were frequently “unsymmetric.” We noted also that particular Na^+ distributions were often rather “long-lived”, in terms of the number of Monte Carlo iterations. This persistence of “asymmetry,” which merits further investigation by molecular dynamics simulation, has undoubtedly contributed to the Na^+ distributions in the top and bottom rows in Figure 2, and evidently is exacerbated by increasing tetrahedral layer charge.

Oxygen (solid curve) and H (dashed curve) density profiles for the same set of model clay-water systems as in Figure 2 are shown in Figure 3. Regardless of layer charge or the degree of tetrahedral substitution, the principal location of the water molecules is at the midplane. The breadth of the O atom peak increases with decreasing layer charge and there is growth as well in the number of water molecules occupying the hexagonal cavities in the siloxane surface (the “wings” of the O atom density profile near $z = 4$ and 8 \AA). X-ray and neutron diffraction analyses of the monolayer hydrate of Wyoming-type montmorillonite place the O atoms of interlayer water molecules principally at $z = 5.8 \pm 0.1 \text{ \AA}$ (Pezerat and Méring 1967, Hawkins and Egelstaff 1980). The breadth of the O and H peaks, both in the MC simulations and in the diffraction experiments, suggests a relatively disordered interlayer water structure, although the neutron diffraction data suggest that some of the water molecules are “spatially correlated with the silicate layers” (Hawkins and Egelstaff 1980). These latter water molecules could be in the hexagonal cavities.

The O and H atom density profile obtained by Skipper *et al* (1991a) for the monolayer hydrate of Na-vermiculite by neutron diffraction is shown alongside the MC simulation result in Figure 3. The quantitative agreement is very good between the two profiles and with previous studies based on X-ray diffraction analysis (Bradley *et al* 1963, Le Renard and Mamy 1971, de la Calle *et al* 1984).

Interlayer coordination environments

Sodium-oxygen radial distribution functions computed from the MC simulations using Eq. (4) are shown

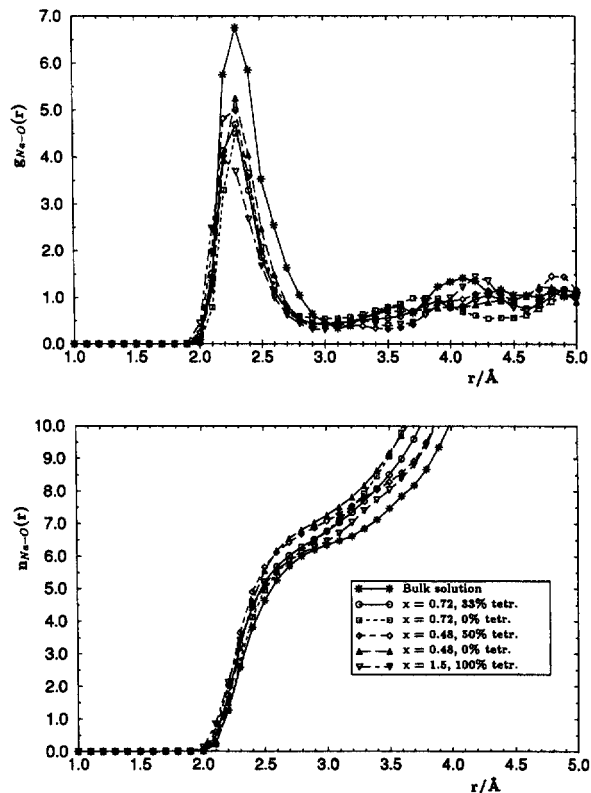


Figure 4. Graphs of $g_{\text{NaO}}(r)$ and $n_{\text{NaO}}(R)$ for Na^+ in bulk solution and interlayer water.

in Figure 4 for the model clay minerals listed in Table 1. For comparison, the RDF for Na^+ in bulk liquid water as calculated from an MC simulation also is presented. The primary peak in the RDF occurs at 2.3 \AA for bulk solution and for the montmorillonites without tetrahedral charge sites, whereas for the clay minerals with tetrahedral charge sites, the peak moves progressively toward 2.2 \AA as the percentage of tetrahedral charge increases. Diffraction experiments on bulk solutions yield a peak position at 2.35 \AA (Skipper and Neilson 1989), while simulations place it in the range $2.29\text{--}2.35 \text{ \AA}$ (Mezei and Beveridge 1981, Chandrasekhar and Jorgensen 1982, Impey *et al* 1983, Bounds 1985). Thus, the present results for bulk solution are in satisfactory agreement with previous studies. The trend with increasing tetrahedral charge suggests direct binding between Na^+ and siloxane surface O atoms, and a corresponding dissimilarity with the coordination structure in bulk solution. Indeed, on the basis of their diffraction experiments with the monolayer hydrate of Na-vermiculite, both de la Calle *et al* (1984) and Skipper *et al* (1991a) have concluded that Na^+ has significant coordination with surface O and that there are only two water molecules in its first coordination sphere.

The running coordination number of O about Na^+ ,

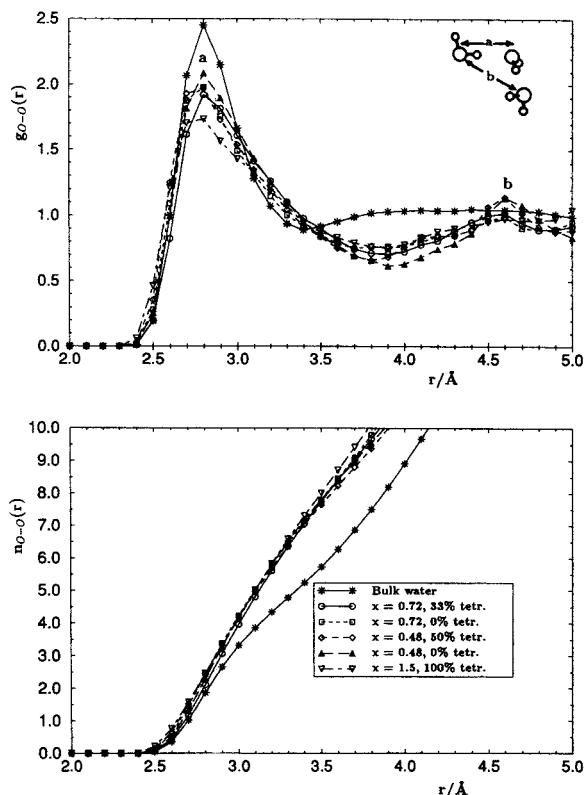


Figure 5. Graphs of $g_{OO}(r)$ and $n_{OO}(R)$ for water molecules in the bulk liquid and in interlayer water.

obtained by integration as in Eq. (5) is shown in the lower half of Figure 4. Within a radius of 3 Å (the position of the first minimum in the RDF), there are six water molecules in the solvation complex of Na^+ in bulk solution, the same number as found typically by experiment or simulation (Bounds 1985). This number increases to seven as the layer charge of the model clay minerals decreases, with the effect of tetrahedral substitution being to retard this increase. Detailed examination of the simulation results reveals that about 60% of the O atoms at the highest coordination number are in water molecules, with the remainder derived from the clay mineral. This percentage declines to about 33% for vermiculite, as stated above. Thus, there are important differences between Na^+ in bulk solution and in interlayer water with respect to the structure of the local coordination environment.

Figure 5 shows the O-O RDF for bulk water and the same five model clay minerals as in Figure 4. In bulk water, $g_{OO}(r)$ indicates the relative placement of water molecules about a reference molecule, with the first peak (denoted *a*) indicating the nearest-neighbor position and the second (denoted *b*), the position of next-nearest neighbors. The first peak is known from diffraction experiments and simulations to occur near 2.8

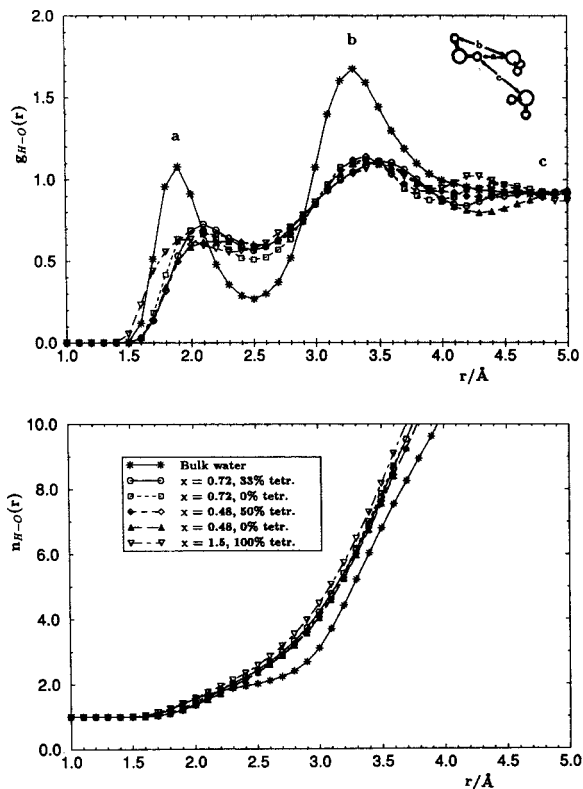


Figure 6. Graphs of $g_{OH}(r)$ and $n_{OH}(R)$ for water O atoms in the bulk liquid and in interlayer water.

Å (Beveridge *et al* 1983), while the broad second peak is centered near 4.5 Å, in agreement with the MC simulation results in the present study. For interlayer water, the two peaks in the O-O RDF occur at these same two values, but the second peak is much better defined than it is for bulk water. The fact that the second peak is at 4.5 Å instead of 5.6 Å ($= 2 \times 2.8$ Å) means that orientational correlations among the water molecules are important; the fact that the second peak is relatively sharper for interlayer water implies that tetrahedral coordination of the water molecules is relatively enhanced (more "ice-like") as compared to bulk water (Beveridge *et al* 1983). The coordination number in the first hydration shell ($R = 3.4$ Å) about a water molecule in the bulk liquid is near five, whereas that for interlayer water molecules is about twice this value at $R = 3.8$ Å (the position of the first minimum in the RDF), irrespective of clay mineral charge characteristics. The larger n_{OO} -value reflects the substantial near presence of clay mineral O atoms to interlayer water molecules.

Figure 6 shows the O-H RDF for the same six systems as in Figure 5. In bulk water, $g_{OH}(r)$ has a peak (denoted *a*), indicating the average O...H hydrogen bond distance to be 1.9 Å, and a second peak (denoted *b*) at 3.3 Å reflecting nearest-neighbor OH spatial cor-

relations (Beveridge *et al* 1983). Given the 104.52° angle between OH bonds of length 0.9572 \AA in a water molecule (Buckingham 1987), linear hydrogen bonds would lead to a second peak in $g_{\text{OH}}(r)$ at $r = 3.2 \text{ \AA}$ (cf. the inset at the upper right in the graph of $g_{\text{OH}}(r)$ in Figure 6). The O-H RDF show maxima at $1.9\text{--}2.3 \text{ \AA}$, $3.4\text{--}3.5 \text{ \AA}$, and $4.3\text{--}5.0 \text{ \AA}$, implying longer hydrogen bonds than in bulk water, but a closer approach of next-nearest-neighbor O to a reference water molecule. The coordination of two H atoms with each O atom in bulk water is apparent from the plot of the running coordination number (lower half of Figure 6, $n_{\text{OH}}(R = 2.5 \text{ \AA}) \approx 2$), while a somewhat larger coordination of H about O occurs in interlayer water. The case of vermiculite is interesting, in that the first two peaks in $g_{\text{OH}}(r)$ appear at the same positions as for bulk water (and with 2 H per O atom), but a *third* peak occurs at 4.3 \AA , indicating close proximity of a next-nearest-neighbor O atom, possibly in the siloxane surface of the clay mineral. This possibility is consistent with hydrogen bonding to the siloxane surface, a conclusion supported by the trend of increasing r -value at the third peak with decreasing layer and/or tetrahedral site charge in the clay mineral.

Additional insight as to the orientations of interlayer water molecules can be obtained by examining the functions $P(\theta)$ and $P(\phi)$ defined in Eqs. (6) and (7). These functions, as computed in the MC simulations for the five model clay minerals described in Figures 2–6, are shown in Figure 7. In order to interpret the graphs, it may be noted that maxima at $\theta = 52^\circ$ and $\phi = 38^\circ$ are expected if a water molecule is oriented as in Figure 1; maxima at $\theta = 90^\circ$ and $\phi = 0^\circ$ are expected if a water molecule orients with its dipole moment vector parallel to the siloxane surface; and maxima at $\theta = 128^\circ$ and $\phi = 38^\circ$ are expected if the molecule orients with its OH bond perpendicular to the siloxane surface opposing the one depicted in Figure 1 (i.e., a counter-clockwise rotation by 75.5° , the supplement of the tetrahedral angle 104.5°). Evidence for all of these orientations can be seen in Figure 7. It appears in addition that the montmorillonites contain interlayer water molecules oriented with their dipole moment vectors perpendicular to the siloxane surface ($\theta = 0^\circ$, $\phi = 90^\circ$). The trend is to favor orientation parallel to the siloxane surface ($\theta = 90^\circ$) as the percentage of tetrahedral charge decreases.

CONCLUSIONS

Monte Carlo simulations of Na-saturated Wyoming-type montmorillonite and vermiculite following the methodology of Skipper *et al* (1994) have yielded layer spacings, average potential energies, and molecular structure information for the dehydrated forms and monolayer hydrates of these clay minerals that are in good semiquantitative to quantitative agreement with a variety of experimental results. This good agreement

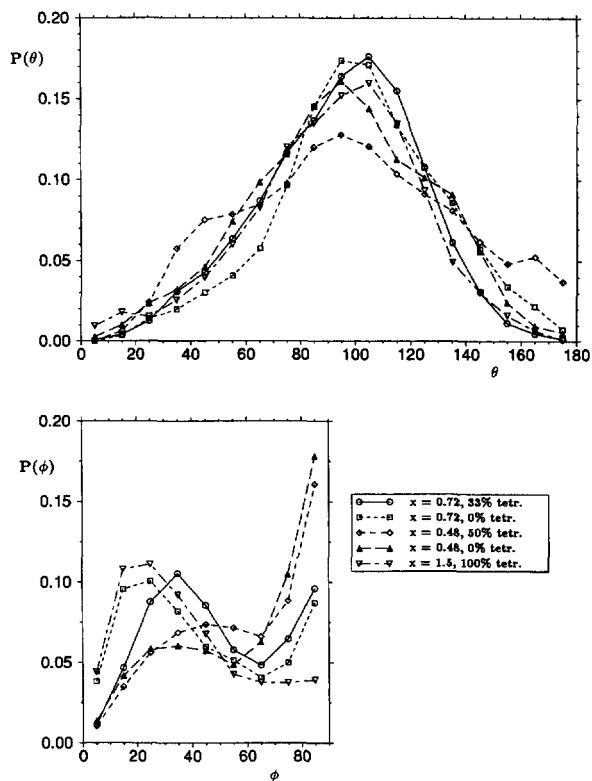


Figure 7. Graphs of $P(\theta)$ and $P(\phi)$ (Equations 6 and 7) for interlayer water in model clay mineral systems (Table 1).

lends credence to the simulation approach adopted and, in particular, to the potential functions utilized to represent water-water, Na^+ -water, and Na^+ /water-clay mineral interactions. The monolayer hydrate offers an especially stern test of these potential functions because its essentially two-dimensional structure differs considerably from that in bulk aqueous solution.

The qualitative picture of interlayer water that emerges from the MC simulations is that of water molecules affected significantly by the magnitude and distribution of layer charge in the clay mineral. As layer charge increases, water molecules tend to increase their occupation of the interlayer midplane and adopt an orientation with their dipole moment vectors parallel to the siloxane surface. As the percentage of tetrahedral layer charge increases, these molecules are induced to interact more with the siloxane surface O atoms (evidently through hydrogen bonding), orienting themselves with an OH directed at an O atom near a tetrahedral site. The effect on adsorbed Na^+ from increasing layer charge or percentage of tetrahedral charge sites is to induce the formation of inner-sphere surface complexes.

Taken as a whole, the MC simulations point to the need for careful X-ray and neutron diffraction experiments on a series of monolayer-hydrate montmoril-

lonites whose layer charge and percentage tetrahedral charge are varied systematically. The pioneering efforts of Pezerat and Méring (1967) and Hawkins and Egelstaff (1980) could be much improved upon by present diffraction technology.

ACKNOWLEDGMENTS

The research reported in this paper was supported in part by NSF grant EAR-9206052. The first author thanks Pembroke College, Cambridge University, and British Gas for their support through the award of the Sir Henry Jones Research Fellowship. Gratitude is expressed to Terri DeLuca for excellent typing of the manuscript and to the San Diego Supercomputer Center for an allocation of Service Units on its Cray Y-MP8/864 supercomputer.

REFERENCES

- Adamson, A. W. 1990. *Physical Chemistry of Surfaces*. New York: Wiley, 591–681.
- Allen, M. P., and D. J. Tildesley. 1987. *Computer Simulation of Liquids*. Oxford: Clarendon Press, 110–139.
- Bailey, S. W. 1980. Structures of layer silicates. In *Crystal Structures of Clay Minerals and their X-ray Identification*. G. W. Brindley and G. Brown, eds. London: Mineralogical Society, 1–123.
- Beveridge, D. L., M. Mezei, P. K. Mehrotra, F. T. Marchese, G. Ravi-Shanker, T. Vasu, and S. Swaminathan. 1983. Monte Carlo computer simulation studies of the equilibrium properties and structure of liquid water. In *Molecular-Based Study of Fluids*. J. M. Haile and G. A. Mansoori, eds. Washington: American Chemical Society, 297–351.
- Bleam, W. F. 1993. Atomic theories of phyllosilicates. *Rev. Geophys.* **31**: 51–73.
- Bopp, P. 1987. Molecular dynamics simulations of aqueous ionic solutions. In *The Physics and Chemistry of Aqueous Ionic Solutions*. M.-C. Bellissent-Funel and G. W. Neilson, eds. Boston: D. Reidel, 217–243.
- Bounds, D. G. 1985. A molecular dynamics study of the structure of water around the ions Li^+ , Na^+ , K^+ , Ca^{2+} , Ni^{2+} , and Cl^- . *Mol. Phys.* **54**: 1334–1355.
- Bradley, W. F., E. J. Weiss, and R. A. Rowland. 1963. A glycol sodium vermiculite complex. *Clays & Clay Miner.* **10**: 117–122.
- Buckingham, A. D. 1987. The structure and properties of a water molecule. In *Water and Aqueous Solutions*. G. W. Neilson and J. E. Enderby, eds. Boston: Adam Hilger, 1–10.
- Chandrasekhar, J., and W. L. Jorgensen. 1982. The nature of dilute solutions of sodium ions in water, methanol, and tetrahydrofuran. *J. Chem. Phys.* **77**: 5080–5089.
- de la Calle, C., and H. Suquet. 1988. Vermiculite. *Rev. Mineral.* **19**: 455–496.
- de la Calle, C., A. Plançon, C. H. Pons, J. Dubernat, H. Suquet, and H. Pezerat. 1984. Mode d'Empilement des Feuilletés dans la Vermiculite Sodique Hydratée à Une Couche (Phase à 11.85 Å). *Clay Miner.* **19**: 563–578.
- Fu, M. H., Z. Z. Zhang, and P. F. Low. 1990. Changes in the properties of a montmorillonite-water system during the adsorption and desorption of water. Hysteresis. *Clays & Clay Miner.* **38**: 485–492.
- Güven, N. 1992. Molecular aspects of clay-water interactions. In *Clay-Water Interface and Its Rheological Implications*. N. Güven and R. M. Pollastro, eds. Boulder: The Clay Minerals Society, 2–79.
- Hawkins, R. K., and P. A. Egelstaff. 1980. Interfacial water structure in montmorillonite from neutron diffraction experiments. *Clays & Clay Miner.* **28**: 9–28.
- Impey, R. W., P. A. Madden, and I. R. McDonald. 1983. Hydration and mobility of ions in solution. *J. Phys. Chem.* **87**: 5071–5083.
- Johnston, C. T., G. Sposito, and C. Erickson. 1992. Vibrational probe studies of water interactions with montmorillonite. *Clays & Clay Miner.* **40**: 722–730.
- Keren, R., and I. Shainberg. 1975. Water vapor isotherms and heat of immersion of Na/Ca-montmorillonite systems—I. Homoionic clay. *Clays & Clay Miner.* **23**: 193–200.
- Keren, R., and I. Shainberg. 1980. Water vapor isotherms and heat of immersion of Na/Ca-montmorillonite systems—III. Thermodynamics. *Clay & Clay Miner.* **28**: 204–210.
- Le Renard, J., and J. Mamy. 1971. Etude de la structure des phases hydratées des phlogopites altérées par des projections de Fourier monodimensionnelles. *Bull. Groupe Français Argiles* **23**: 119–127.
- Low, P. F. 1985. The clay-water interface. *Proc. Int. Clay Conf.*, Denver: Clay Minerals Society, 247–256.
- Low, P. F. 1987. Structural component of the swelling pressure of clays. *Langmuir* **3**: 18–25.
- Madden, P. A., and R. W. Impey. 1986. Dynamics of coordinated water: A comparison of experiment and simulation results. *Ann. N.Y. Acad. Sci.* **482**: 91–114.
- Matsouka, O., E. Clementi, and M. Yoshimine. 1976. CI study of the water dimer potential surface. *J. Chem. Phys.* **64**: 1351–1361.
- Mezei, M., and D. L. Beveridge. 1981. Monte Carlo studies of the structure of dilute aqueous solutions of Li^+ , Na^+ , K^+ , F^- , and Cl^- . *J. Chem. Phys.* **74**: 6902–6910.
- Miller, S. E., and P. F. Low. 1990. Characterization of the electrical double layer of montmorillonite. *Langmuir* **6**: 289–296.
- Mooney, R. W., A. G. Keenan, and L. A. Wood. 1952a. Adsorption of water vapor by montmorillonite. I. Heat of desorption and application of BET theory. *J. Am. Chem. Soc.* **74**: 1367–1371.
- Mooney, R. W., A. G. Keenan, and L. A. Wood. 1952b. Adsorption of water vapor by montmorillonite. II. Effect of exchangeable ions and lattice swelling as measured by X-ray diffraction. *J. Am. Chem. Soc.* **74**: 1371–1374.
- Newman, A. C. D. 1987. The interaction of water with clay mineral surfaces. In *Chemistry of Clays and Clay Minerals*. A. C. D. Newman, ed. New York: Wiley, 237–274.
- Newman, A. C. D., and G. Brown. 1987. The interaction of water with clay mineral surfaces. In *Chemistry of Clays and Clay Minerals*. A. C. D. Newman, ed. New York: Wiley, 1–128.
- Pezerat, H., and J. Méring. 1967. Recherches sur la position des cations échangeables et de l'eau dans les montmorillonites. *C.R. Acad. Sci. Paris* **265** (Série D): 529–532.
- Schulz, L. G. 1969. Lithium and potassium adsorption, dehydroxylation temperature, and structural water content of aluminous smectites. *Clays & Clay Miner.* **17**: 115–149.
- Skipper, N. T. 1992. *MONTE: User's Manual*: Technical Report, Department of Chemistry, University of Cambridge, UK.
- Skipper, N. T. and G. W. Neilson. 1989. X-Ray and neutron diffraction studies on concentrated aqueous solutions of sodium nitrate and silver nitrate. *J. Phys. Condens. Matter* **1**: 4141–4154.
- Skipper, N. T., K. Refson, and J. D. C. McConnell. 1989. Computer calculation of water-clay interactions using atomic pair potentials. *Clay Miner.* **24**: 411–425.
- Skipper, N. T., A. K. Soper, and J. D. C. McConnell. 1991a.

- The structure of interlayer water in vermiculite. *J. Chem. Phys.* **94**: 5751–5760.
- Skipper, N. T., K. Refson, and J. D. C. McConnell. 1991b. Computer simulation of interlayer water in 2:1 clays. *J. Chem. Phys.* **94**: 7434–7445.
- Skipper, N. T., K. Refson, and J. D. C. McConnell. 1993. Monte Carlo simulations of Mg- and Na-smectites. In *Geochemistry of Clay-Pore Fluid Interactions*. D. C. Manning, P. L. Hall, and C. R. Hughes, eds. London: Chapman and Hall, 40–59.
- Skipper, N. T., F.-R. C. Chang, and G. Sposito. 1995. Monte Carlo simulation of interlayer molecular structure in swelling clay minerals. I. Methodology. *Clays & Clay Miner.* (in review).
- Slabaugh, W. H. 1959. Adsorption characteristics of homoionic bentonites. *J. Phys. Chem.* **63**: 436–438.
- Sposito, G. 1984. *The Surface Chemistry of Soils*. New York: Oxford University Press, 1–77.
- Sposito, G. 1992. The diffuse-ion swarm near smectite particles suspended in 1:1 electrolyte solutions: Modified Gouy-Chapman theory and quasicrystal formation. In *Clay-Water Interface and its Rheological Implications*. N. Güven and R.M. Pollastro, eds. Boulder: The Clay Minerals Society, 128–155.
- Sposito, G., and R. Prost. 1982. Structure of water adsorbed on smectites. *Chem. Rev.* **82**: 553–573.
- Sposito, G., R. Prost, and J. P. Gaultier. 1983. Infrared spectroscopic study of adsorbed water on reduced-charge Na/Li montmorillonites. *Clays & Clay Miner.* **31**: 9–16.
- van Olphen, H. 1965. Thermodynamics of interlayer adsorption of water in clays. I. Na vermiculite. *J. Colloid & Interface Sci.* **20**: 822–837.
- Zettlemoyer, A. C., G. J. Young, and J. J. Chessick. 1955. Studies of the surface chemistry of silicate minerals. III. Heats of immersion of bentonites in water. *J. Phys. Chem.* **59**: 962–966.

(Received 9 September 1993; accepted 9 September 1994; MS 2414)